Absolute generalized oscillator strengths of 2 ^1S and 2 ^1P excitations of helium measured by angle-resolved electron-energy-loss spectroscopy

K. Z. Xu, R. F. Feng, S. L. Wu, Q. Ji, X. J. Zhang, and Z. P. Zhong
Department of Modern Physics, University of Science and Technology of China, Hefei, Anhui 230027, China

Y. Zheng
Department of Chemistry, The University of British Columbia, 2036 Main Mall, Vancouver, British Columbia, Canada V6T 1Z1

(Received 2 October 1995; revised manuscript received 26 December 1995)

The differential scattering cross sections and the generalized oscillator strengths of the 1 $^1S \rightarrow 2\ ^1S$ and 1 $^1S \rightarrow 2\ ^1P$ transitions of helium have been measured by angle-resolved electron-energy-loss spectroscopy with an incident electron energy of 1500 eV and within the range 2°–11.5° of scattering angles. The corrections for angular factors and density effects have also been made for the experimental results. The differential cross sections and generalized oscillator strength values are absolute and are the first to be measured at such a high impact energy. The experimental results are compared with other measurements and theoretical calculations in the literature.

PACS number(s): 32.70.Cs, 34.80.Dp

I. INTRODUCTION

Electron-energy-loss spectroscopy (EELS) is a powerful tool for investigating the structure of atomic and molecular energy levels and electron-induced processes. The transfer of energy and momentum from the incident electron to the target can be used to produce both dipole and nondipole electronic transitions. According to the Bethe theory [1], the differential cross section (DCS) for a fast electron impact can be factorized into a factor involving the kinematics of the electron before and after the collision and the transition probability of the resulting excitation of the target, the so-called generalized oscillator strength (GOS), by the following Bethe-Born formula [2,3]:

$$f(W,K)=\frac{W}{2}\frac{p_0}{p_a}K^2\frac{d\sigma}{d\Omega}. \tag{1}$$

Here $f(K,W)$ and $d\sigma/d\Omega$ stand for GOS and DCS, respectively. W and K are the energy loss and the momentum transfer while p_0 and p_a are the incident and scattered electron momentum, respectively. All quantities in Eq. (1) are in atomic units. The atomic unit of energy is hartrees.

The multichannel quantum defect theory can calculate a unique energy-dependent quantum defect as well as the corresponding absolute oscillator strength densities for each particular initial- and final-state combination including the bound and continuous states [4–7]. It provides a powerful tool in predicting the electronic excitation spectrum and the differential cross section. Therefore, a large amount of the data of the excitation cross sections by the electron impact, especially for high excitation states, can be obtained by the interposition from a few of the measured GOS densities.

Many earlier EELS studies have been devoted to measurements of DCS at low impact energies [8] or to measurements of optical oscillator strength (OOS) in a simulation of photoabsorption by high impact energy at near-zero degree forward scattering angle [9–11]. A further development of EELS is angle-resolved EELS (AREELS), in which the scattering angle, i.e., momentum transfer K, is varied. AREELS can be used to measure the absolute DCS and GOS of both dipole and nondipole electronic transitions [3,12]. Absolute GOS measurements as a function of momentum transfer K over an extended range of K values provide additional information about the nature of electronic transitions and of electron scattering processes. They can also provide an effective test of the wave-function models used for both the ground and excited states and of quantum computational methods, since such a GOS profile is directly related to the initial-state and excited-state wave functions.

Electron impact processes of helium are important for both practical and theoretical interests. They exist in various discharge and laser systems, fusion plasmas, the atmosphere, and in stellar objects. They represent one of the simplest inelastic electron scattering processes that are suitable for theoretical treatment and for developing or refining calculational schemes.

A large number of cross-section calculations and measurements have been reported for helium. Most of them gave the DCS at lower incident electron energy as summarized in the reviews of Bransden and McDowell [8] through 1977 and in the papers of Cartwright *et al.* [13] and Trajmar *et al.* [14] more recently. The experimental DCS research of the 2 ^1P and 2 ^1S excitations from the ground state 1 ^1S in helium, in which the energy of incident electrons is greater than 100 eV, is summarized in Table I. This research indicates that the differences between the various theoretical and experimental results and among experimental results are significant.

Kim and Inokuti [25] calculated the first Born approximation results for these two transitions. The earliest authors who indicated that the Born approximation is grossly inadequate at high incident energy and large scattering angle to describe the DCS's of electron scattering were Geltman and Hidalgo [26] for hydrogen and Holt and Moiseiwitsch [27] for helium. Opal and Beaty [20] studied the angular trend of electron scattering by helium at an incident energy of 200 eV and confirmed the essential correctness of the theory. However, due to poor resolution they used unresolved spectra and

TABLE I. Summary of DCS measurements for the $2\,^1P$ and $2\,^1S$ transitions in He.

Reference	Levels	Energy range (eV)	Angular range (deg)	K^2 (units of a_0^{-2})
[15]	$2\,^1S$,$2\,^1P$	511	3.8–8.8	0.18–0.88
[16]	$2\,^1S$,$2\,^1P$	500	9.3–15.3	0.45–2.56
[17]	$2\,^1S$	500	0.5–2.5	0.02–0.09
[18]	$2\,^1P$	400	1.5–4.0	0.04–0.16
[19]	$2\,^1S$,$2\,^1P$	300,400	5.7.5,10	0.19–0.89
[20]	$2\,^1S$,$2\,^1P$	82,200	30–150	3.8–52
[21]	$2\,^1S$,$2\,^1P$	500	5,10,15,20	0.29–4.36
[22]	$2\,^1S$,$2\,^1P$	50–500	20–120	4.36–108
[23]	$2\,^1S$,$2\,^1P$	200–700	7.5–35	0.88–4.70
[24]	$2\,^1S$	200–1000	0–16	0.00–5.65
[13]	$2\,^1P$	30–100	5–140	0.14–23.1
[14]	$2\,^1S$	30–100	10–135	0.29–22.5
This work	$2\,^1S$,$2\,^1P$	1500	2–11.5	0.14–4.40

separated scattering curves for these two transitions by deconvolution. After that Hidalgo and Geltman [28] applied their Coulomb projected Born approximation [26] to these two transitions of helium and significantly reduced the disagreement of the previous theory [25] with experiment [20]. Dillon and Lassettre [23] used fully resolved spectra, extended the measurements to higher incident energies (up to 700 eV), and first determined absolute DCS and GOS of these two transitions. Their experimental results showed that beyond $K^2=5$ the experimental GOS values had large deviations from the Born approximation for the $1\,^1S\rightarrow 2\,^1P$ transition, but at low momentum transfer ($K^2<2.5$) the experimental values had small deviations of 7% to 15% from the first Born approximation. However, for the $1\,^1S\rightarrow 2\,^1S$ transition, even at low momentum transfer, the experimental values still deviate from the first Born approximation curve. Agreement with the Coulomb Born approximation [28] is good but calculated values were higher at larger K^2 for the $1\,^1S\rightarrow 2\,^1P$ transition. Furthermore, their GOS values at higher incident energy and larger momentum transfer were much lower than the measurements by Opal and Beaty [20] and Suzuki, Takayanagi, and Wakiya [22] for both transitions. Moreover, Sakai *et al.* [24] determined relative DCS's for the $2\,^1S$ transition with respect to the $2\,^1P$ at small scattering angles and in the impact energy range 200–1000 eV. They found that the cross section increased as the scattering angle decreased to 0°. Recently Trajmar *et al.* [14] confirmed again this conclusion at lower impact energy range 30–100 eV. On the other hand, in previous experiments with high impact energies, these two transitions were usually not resolved due to poor energy resolution [29,30].

So far there have been few theoretical and experimental results for higher incident energy (more than 700 eV) and larger momentum transfer. Therefore further studies of inelastic electron scattering by helium at higher incident energy and larger momentum transfer are needed both experimentally and theoretically.

In this paper, our recent experimental results for the DCS and GOS for the $1\,^1S\rightarrow 2\,^1S$ and $1\,^1S\rightarrow 2\,^1P$ transitions in helium measured at an incident electron energy of 1500 eV and scattering angles within the range 2°–11.5° are reported. The DCS and GOS values are absolute and are the first to be measured at such a high impact energy. Under such a condition, the first Born approximation is closer to being valid, so the GOS values we measured are considered to be closer to real GOS values. The present experimental measurements are compared with previous experimental and theoretical results.

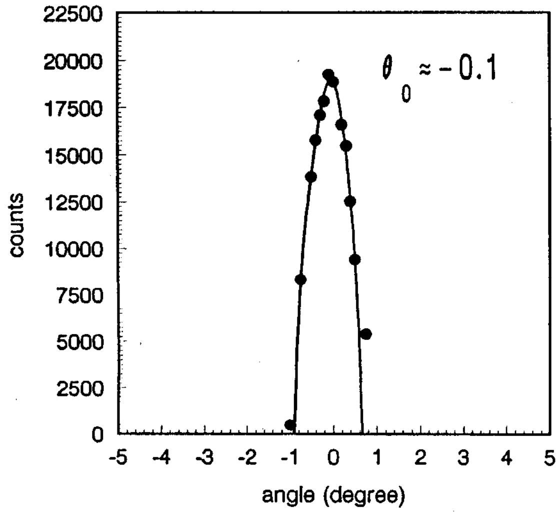

FIG. 1. Calibration for the scattering angles. The horizontal axis represents the geometric angle of the spectrometer.

II. EXPERIMENTAL APPARATUS AND PROCEDURES

The electron impact apparatus used to obtain the data of helium in this work is a recently built angle-resolved double hemispherical electron energy-loss spectrometer. Details of the apparatus were described in our previous work [11]. Briefly it consists of an electron gun, a hemispherical electrostatic monochromator made of aluminum, a rotatable energy analyzer of the same type, an interaction chamber, a number of cylindrical electrostatic optics lens, and a channeltron for detecting the analyzed electrons. All of these components are enclosed in four separate vacuum chambers made of stainless steel. Pulse-counting and multiscaler techniques were used to obtain energy-loss spectra.

It is known that angular accuracy has a great influence on observed signal intensities, particularly in the case of forward scattering. The scattering angles (θ) were calibrated based on the symmetry of the $1\,^1S\rightarrow 2\,^1P$ inelastic scattering signal around the geometric nominal zero angle. Figure 1 gives the result of this measurement and shows that the true scattering angle is 0.1° less than the geometric zero angle of the spectrometer. The angular resolution of the spectrometer has been approximately determined from the angular distribution of the direct electron beam from the monochromater by rotating the energy analyzer. It is shown in Fig. 2. The angular resolution is about 0.6° [full width at half maximum (FWHM)], which is good enough for the present measurements.

The impact energy of the spectrometer can be varied from 1 to 5 keV and the energy resolution is 40–120 meV (FWHM). These variables were set up at 1.5 keV and 120

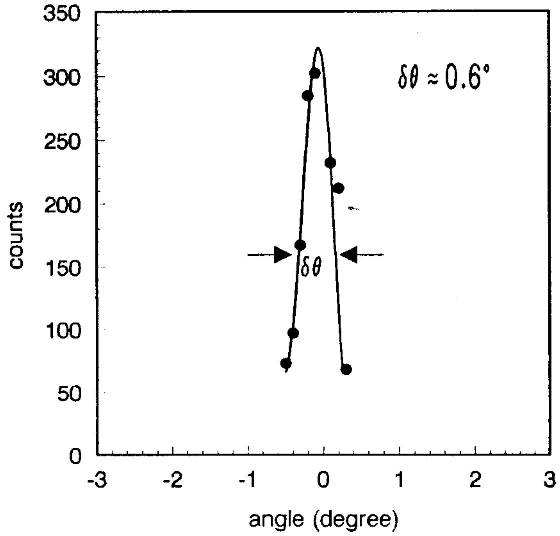

FIG. 2. Angular resolution of the spectrometer.

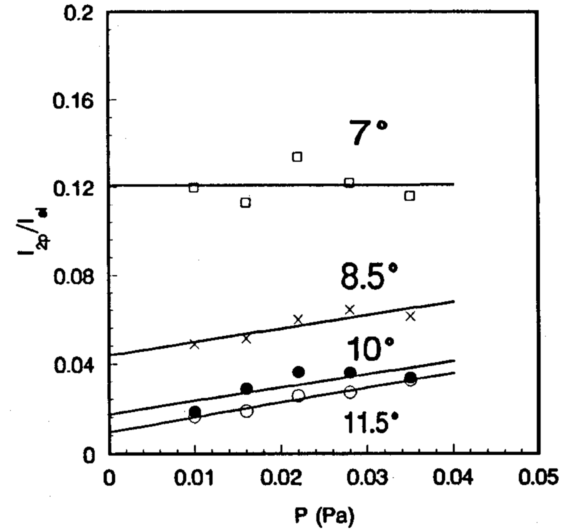

FIG. 3. Intensity ratios I_P/I_{el} as a function of pressure.

meV for the present measurements.

It should be considered that two types of double scattering processes are the principal causes of errors in DCS measurements of inelastic scattering at large scattering angles θ [31]. First, an electron, inelastically scattered at an angle α, is elastically scattered at an angle $\theta-\alpha$. Second, an elastically scattered electron at an angle β is followed by inelastic scattering at an angle $\theta-\beta$.

To decrease the path length of electrons through the atomic gas with high density, there is a gas cell with differential pumping in the center of the interaction chamber. The length of the cell is 24 mm and the atomic helium gas goes directly into the cell. The background pressure in the vacuum chambers was 2.2×10^{-7} Torr. The shorter collision cell and lower pressure help decrease the effects due to the two types of double scattering processes on DCS measurements at larger scattering angles for the $1\,^1S\rightarrow2\,^1P$ transition. In order to evaluate and eliminate the effect, we measured the pressure relation of the intensity ratios for the $1\,^1S\rightarrow2\,^1S$ and $1\,^1S\rightarrow2\,^1P$ transitions and also for elastic scattering at all scattering angles. Because the cross section of double scattering process depends on the square of the pressure (or density) of measured gas, but the cross section of the single scattering process depends on pressure, and also because the cross section of the elastic scattering is much more than that of inelastic scattering at large scattering angle, there is an approximate relation between the measured intensity ratios and the pressure P as follows [23]:

$$I_P/I_{\mathrm{el}}=(I_P/I_{\mathrm{el}})_{P=0}+cP, \tag{2}$$

where I_P and I_{el} represent the scattering intensities corresponding to the $2\,^1P$ excitation and elastic scattering, respectively, including single and double scatterings. The intensity ratios as a function of pressure at some angles are shown in Fig. 3. $(I_P/I_{\mathrm{el}})_{P=0}$ is the intensity ratio extrapolated to zero gas pressure. As to a different angle, there is a different ratio of $(I_P/I_{\mathrm{el}})_{P=0}$ to $(I_P/I_{\mathrm{el}})_P$ for different pressure. Multiplying the ratio and the inelastic scattering intensity after the correction of instability of beam current, it is a true relative inelastic scattering intensity without pressure effect. The lines used to obtain the $(I_P/I_{\mathrm{el}})_{P=0}$ in Fig. 3 are the least-square fits to the data points. The slope of the line is the constant c in the formula (2). It is obvious that the correction for the pressure effect becomes weak when the scattering angle is less than 8.5°. We also measured the pressure relation of the ratios of the $1\,^1S\rightarrow2\,^1S$ transition for all angles. It was found that there was no need to correct the pressure effect for the $1\,^1S\rightarrow2\,^1S$ transition. Therefore, the DCS's of the $2\,^1P$ transition in Table II have been corrected for pressure effects only at the angles greater than 7°. The pressure effect for the remaining DCS's was negligible.

In the collision cell case, the scattered electrons go out not from a "point," but for a "line." The scattering length seen by the energy analyzer at a scattering angle θ is proportional to $1/\sin\theta$ at larger scattering angles [32]. But at smaller scattering angles it does not increase further because of the fixed length of the collision cell. In order to get the true angular distribution of scattered electrons, it is necessary to calibrate the angular factor of our apparatus to correct the "line source" and other effects.

The experiment of Dillon and Lassettre [23] at an incident energy of 700 eV in the K^2 range 0.88–4.7 has shown that the relative differences of the summed GOS values of the

TABLE II. Angular factor.

θ (deg)	K^2 (a.u.)	$\frac{d\sigma}{d\Omega}$ [a] ($10^{-2}a_0^2$ sr^{-1})	I	$\frac{d\sigma}{d\Omega}\Big/I$	$\frac{\sin\theta}{\sin7°}$	$A(\theta)$
2	0.139	423	1110	0.381	0.286	0.389
3	0.306	156	306	0.510	0.429	0.498
4	0.539	68.0	111	0.613	0.572	0.612
5.5	1.01	22.1	28.3	0.781	0.786	0.786
7	1.64	7.56	7.56	1	1	1
8.5	2.41	2.84	2.22	1.28	1.21	1.21
10	3.33	1.10	0.724	1.52	1.42	1.42
11.5	4.40	0.443	0.275	1.61	1.64	1.64

[a]Reference [25].

TABLE III. The GOS and DCS for the $1\,^1S\rightarrow 2\,^1P$ and $1\,^1S\rightarrow 2\,^1S$ excitations of helium.

K^2 (units of a_0^{-2})	0.139	0.306	0.539	1.01	1.64	2.41	3.33	4.40
				$2\,^1P$				
GOS (units of 10^{-2})								
This work	24.1	17.2	12.6	6.99	3.33	1.40	0.616	0.314
Ref. [23]			10.4	5.81	2.67	1.12	0.532	0.261
Ref. [25]	22.1	17.1	12.2	6.47	3.06	1.37	0.593	0.255
DCS ($10^{-2}a_0^2\,\mathrm{sr}^{-1}$)								
This work	442	144	55.7	17.6	5.17	2.57	0.471	0.182
				$2\,^1S$				
GOS (units of 10^{-2})								
This work	1.05	1.68	2.07	2.13	1.70	1.18	0.748	0.471
Ref. [23]			2.11	1.88	1.49	1.03	0.640	0.406
Ref. [25]	0.949	1.65	2.14	2.24	1.82	1.28	0.818	0.496
DCS ($10^{-2}a_0^2\,\mathrm{sr}^{-1}$)								
This work	20.7	14.3	9.42	5.52	2.72	1.29	0.589	0.280

$1\,^1S\rightarrow 2\,^1S$ and $1\,^1S\rightarrow 2\,^1P$ transitions between their experiment and the calculation by Kim and Inokuti [25] are less than $\pm 4\%$. The experiments of Wong, Lee, and Bonham [29] at an incident energy of 25 KeV and in the K^2 range 0.25–5 and of Ying *et al.* [30] at an incident energy of 2.5 keV and in the K^2 range 0.02–4.7 have also shown that the agreement between their experiments and the calculations of Kim and Inokuti is excellent. Therefore, our angular factor $A(\theta)$ was obtained by dividing the DCS values obtained from Kim and Inokuti [25] by the measured summed counts for these two transitions at different angles with the results being normalized at an angle of 7°.

Column 3 in Table II shows the summed DCS's of these two transitions calculated from the GOS of Kim and Inokuti. Column 4 shows the measured relative summed counts I of the peaks corresponding to these two transitions normalized to column 3 at 7°. The effect of double scattering processes has been corrected in the counts. Column 5 shows ratios that were got by dividing column 3 by column 4. Column 6 shows $\sin\theta\sin 7°$ normalized at 7°.

Comparing column 5 and column 6, one can see that the values are in agreement in larger angular range, but their differences are bigger at smaller angles because of the above-mentioned fixed length of the gas cell. Therefore, we took $\sin\theta$ at angles of 5.5° and higher and took the fitted values from the experimental data points at smaller angles as the angular factor $A(\theta)$ shown in column 7.

III. RESULTS AND DISCUSSION

To determine DCS's and GOS's of the $1\,^1S\rightarrow 2\,^1S$ and $1\,^1S\rightarrow 2\,^1P$ excitations of helium, a number of electron energy-loss spectra were measured at a series of scattering angles (corresponding to different momentum transfer values) sequentially in repetitive scans by above spectrometer. These scattering angles are 2°, 3°, 4°, 5.5°, 7°, 8.5°, 10°, and 11.5°. The spectra were recorded primarily at an incident energy of 1500 eV and a scanning energy region of 2.56 eV including these two excitations. In order to correct the effect of double scattering processes, the EELS of the series of scattering angles were measured at five different values of pressure.

There is some small change in the intensity of the incident electron beam during the measuring period. In order to minimize this systematic error, each time an elastic and inelastic EELS was measured at an angle, the EELS at an angle of 2° was measured alternately. Every measured count of the peak of both elastic and inelastic scattering was normalized to that of the $2\,^1P$ excitation at 2°.

Subtracting backgrounds, correcting for the instability of beam current and the effects of double scattering processes, and multiplying the corresponding angular factors $A(\theta)$ at every angle, we obtained the relative DCS's for these two transitions. The relative GOS's were obtained from the Bethe-Born formula (1) and then were put on an absolute scale using the following method. For sufficiently high incident electron energy, where the first Born approximation is valid, the apparent GOS should be equal to the real GOS. Furthermore, the OOS is approached from the GOS by approaching the limit $K^2\rightarrow 0$. The obtained relative GOS's of the $2\,^1P$ excitation were extrapolated to $K^2\rightarrow 0$ by the following formula [33]:

$$f(K,E)=\frac{1}{(1+x)^6}\sum_{n=0}^{m} f_n\left(\frac{x}{1+x}\right)^n, \qquad (3)$$

where $x=(K/\alpha)^2$, $\alpha=(2I)^{1/2}+[2(I-W)]^{1/2}$, I is the first ionization energy, f_0 is the OOS. The GOS value of the $1\,^1S\rightarrow 2\,^1P$ transition at $K=0$ should be the OOS value that has been measured using our EELS spectrometer at an angle of 0° and is 0.280 [34]. The absolute GOS's for these two transitions were then obtained and are shown in Table III and Fig. 4 respectively. The absolute DCS's for these two transitions can be obtained from formula (1) and are shown in Table III and Fig. 5.

The overall percentage error of the DCS's and GOS's obtained in the present work came from the statistics of counts δ_s, the angular determination and the angular factor [35] δ_a the measured OOS value with systematic error δ_0, and the pressure correction δ_p. In our measurement the

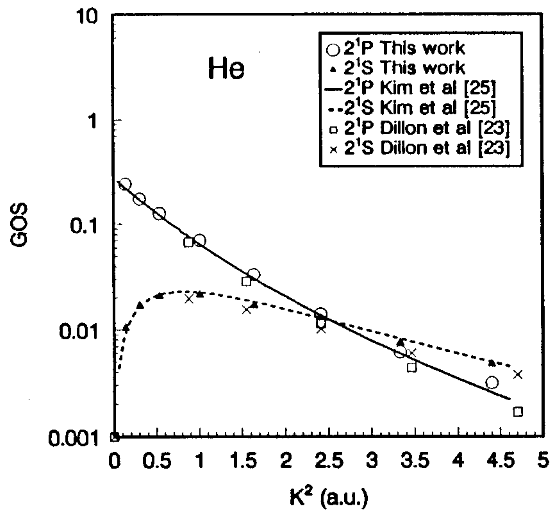

FIG. 4. Absolute GOS's of the $2\,^1P$ and $2\,^1S$ excitations (present, Ref. [23], Ref. [25]).

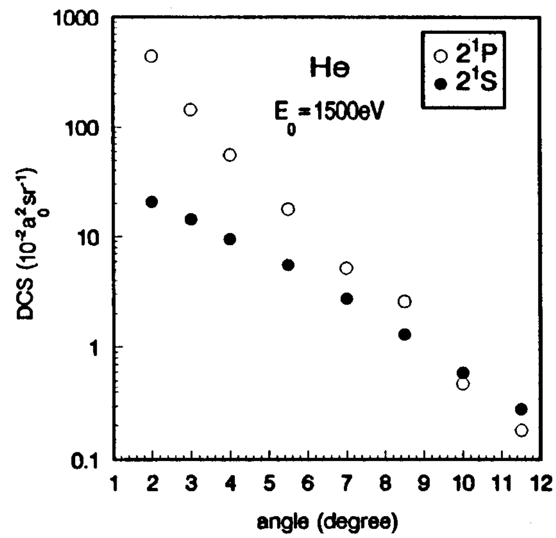

FIG. 5. Absolute DCS's of the $2\,^1P$ and $2\,^1S$ excitations.

maximum of each error is $\delta_s=3\%$, $\delta_a=4\%$, $\delta_0=6\%$, and $\delta_p=2\%$. The total error is less than 8%.

Table III and Fig. 4 also give the GOS values for the $2\,^1P$ and $2\,^1S$ excitations calculated using the Born approximation by Kim and Inokuti [25] and measured by Dillon and Lassettre at an incident energy of 700 eV [23]. All of the values of Kim and Inokuti, and Dillon and Lassettre in Table III are from the least-square fits to their data. In Fig. 4 the solid line and the dotted line represent the theoretically calculated results of these two transitions, respectively. Hidalgo and Geltman [28] calculated the DCS and GOS values at an incident energy of 1500 eV but K^2 are more than 7.4.

There are only a few experimental results for the GOS and DCS for these two transitions [19,23] that used incident electron energies in excess of 400 eV and momentum transfer K^2 more than 1. Vriens, Simpson, and Mielczarek [19] used an electron energy of 400 eV, but a scattering angle less than 10° ($K^2<0.9$). Dillon and Lassettre [23] used the highest electron energy of 700 eV and scattering angles of 7.5°, 10°, 12.5°, 15°, and 17.5° ($K^2=0.88$–4.70). Their DCS and GOS values for the $2\,^1P$ transition are absolute and were calibrated using the elastic DCS's measured by Bromberg at the same incident energy and scattering angles [36]. The total error is 6%. Silverman and Lassettre [16] used an incident energy of 500 eV and scattering angles within the range 6.3°–15.3° ($K^2=0.45$–2.56) for the $2\,^1P$ transition and 9.3°–15.3° for the $2\,^1S$ transition. Their DCS and GOS values for the $2\,^1P$ transition are relative and were normalized to a Born approximation calculation [37]. The DCS and GOS values of the $2\,^1S$ transition for above-mentioned research were normalized by comparison to the absolute values of the $2\,^1P$ transition.

So up to now the highest incident electron energy used to measure the DCS and GOS of the $2\,^1P$ and $2\,^1S$ excitations of He is 700 eV [23]. But their smallest K^2 value is 0.88. What we can compare with previous results is GOS values. The results of Dillon and Lassettre are about 10–20% lower than ours for both the $2\,^1S$ and $2\,^1P$ excitations except at $K^2=0.539$ for the $2\,^1S$ excitation. Their GOS values at $K^2=0.539$ are extrapolated. Compared with the calculated results of Kim and Inokuti [25], our results are in agreement with theirs for both transitions.

Table IV gives several values of the point of intersection of θ and K^2 of two GOS curves for the $1\,^1S\rightarrow2\,^1P$ and $1\,^1S\rightarrow2\,^1S$ transitions. They were obtained by least-square fits to the data. Table IV also gives several θ and K^2 values corresponding to the maximum of the GOS curve for the $2\,^1S$ transition. The largest K^2 in Ref. [16] is 2.56 and their intersection value in Table IV is an extrapolated value by us.

TABLE IV. The point of intersection of two GOS curves for the $2\,^1P$ and $2\,^1S$ excitations and the maxima of the GOS curve for the $2\,^1S$ excitation.

	Experimental						Theoretical
	Ours	Ref. [23]	Ref. [16]	Ref. [21]	Ref. [20]	Ref. [14]	Ref. [25]
E_0 (eV)	1500	700	500	500	200	100	
Intersection							
θ (deg)	9.0	13	16	16	35	64	
K^2 (units of a_0^{-2})	2.7	2.6	2.8	2.8	5.1	7.4	2.6
Maximum							
θ (deg)	4.7	<7.5	<9.3			14	
K^2 (units of a_0^{-2})	0.76	<0.88	<0.20			0.48	0.82

Reference [21] did not give separate values of DCS's for these two transitions, but gave their ratios. The point of intersection is corresponding to the ratio being equal to unity. The smallest K^2 in Refs. [23] and [16] are 0.88 and 0.20, respectively. The GOS values $1\,^1S \rightarrow 2\,^1S$ transitions still increase while the K^2 decreases to the smallest values. We give only the smallest θ and K^2. The real maxima should be less than these values. The errors in Ref. [20] are so big that the K^2 value corresponding to the maximum cannot be given accurately. The only theoretical result was obtained by Kim and Inokuti [25].

Our measured intersection value is 2.7. It is obvious from Table IV that the intersection value of K^2 decreases at first and then approaches a constant as the incident electron energy increases. The constant approaches the calculated value of 2.6 by Kim and Inokuti [25].

The K^2 value corresponding to the maximum of the GOS curve for the $2\,^1S$ transition in Ref. [14] is much smaller than ours. The incident electron energy used by them was 100 eV and was too small to get the GOS values. Their GOS values were calculated by us and were apparent. Their results are only for reference. Our measured maximum is 0.76 and is in agreement with the calculated result by Kim and Inokuti. The results of Refs. [16,23] are much lower than ours.

The agreements of our results with Kim and Inokuti for two GOS curves, the K^2 intersection of two GOS curves for the $2\,^1S$ and $2\,^1P$ excitations and the K^2 value corresponding to the maximum of the GOS curve for the $2\,^1S$ excitation show that the first Born approximation is correct at such high incident electron energy and within the range of momentum transfer used by us.

ACKNOWLEDGMENTS

Financial support for this work was provided by the National Natural Science Foundation of China. We wish to express our sincere thanks to Professor J. M. Li and Professor C. E. Brion for useful discussions. One of the authors, K. Z. X. gratefully acknowledges the support of K. C. Wong Education Foundation, Hong Kong.

[1] H. Bethe, Ann. Phys. **5**, 325 (1930); Z. Phys. **76**, 293 (1932).
[2] M. Inokuti, Rev. Mod. Phys. **43**, 297 (1971).
[3] R. A. Bonham, *Electron Spectroscopy: Theory, Techniques and Applications*, edited by C. R. Brundle and A. D. Baker (Academic, New York, 1979), Vol. 3, p. 127.
[4] M. J. Seaton, Rep. Prog. Phys. **46**, 167 (1983).
[5] J.-M. Li, Acta Phys. Sin. **29**, 419 (1980).
[6] B.-G. Tian and J.-M. Li, Acta Phys. Sin. **33**, 1401 (1984).
[7] K.-H. Sze, C. E. Brion, X.-M. Tong, and J.-M. Li, Chem. Phys. **115**, 433 (1987).
[8] B. H. Bransden and M. R. C. McDowell, Phys. Rep. **46**, 249 (1978).
[9] J. W. Gallagher, C. E. Brion, J. A. R. Samson, and P. W. Langhoff, J. Phys. Chem. Ref. Data **17**, 9 (1988).
[10] W. F. Chan, G. Cooper, and C. E. Brion, Phys. Rev. A **44**, 186 (1991).
[11] S. L. Wu, Z. P. Zhong, R. F. Feng, S. L. Xing, B. X. Yang, and K. Z. Xu, Phys. Rev. A **51**, 4494 (1995).
[12] E. N. Lassettre and A. Skerbele, *Methods of Experimental Physics*, edited by D. Williams (Academic, New York, 1974), Vol. 3, Pt. B, p. 868.
[13] D. C. Cartwright, G. Csanak, S. Trajmar, and D. F. Register, Phys. Rev. A **45**, 1602 (1992).
[14] S. Trajmar, D. F. Register, D. C. Cartwright, and G. Csanak, J. Phys. B **25**, 4889 (1992).
[15] E. N. Lassettre, M. E. Krasnow, and S. Silverman, J. Chem. Phys. **40**, 1242 (1964).
[16] S. M. Silverman and E. N. Lassettre, J. Chem. Phys. **40**, 1265 (1964).
[17] A. Skerbele and E. N. Lassettre, J. Chem. Phys. **45**, 1077 (1966).
[18] E. N. Lassettre, A. Skerbele, and V. D. Meyer, J. Chem. Phys. **45**, 3214 (1966).
[19] L. Vriens, J. A. Simpson, and S. R. Mielczarek, Phys. Rev. **165**, 7 (1968).
[20] C. B. Opal and E. C. Beaty, J. Phys. B **5**, 627 (1972).
[21] A. Skerbele, W. R. Harshbarger, and E. N. Lassettre, J. Chem. Phys. **58**, 4285 (1973).
[22] H. Suzuki, T. Takayanagi, and K. Wakiya (unpublished).
[23] M. A. Dillon and E. N. Lassettre, J. Chem. Phys. **62**, 2373 (1975).
[24] Y. Sakai, T. Y. Suzuki, B. S. Min, T. Takayanagi, K. Wakiya, and H. Suzuki, Phys. Rev. A **43**, 1656 (1991).
[25] Y. K. Kim and M. Inokuti, Phys. Rev. **175**, 176 (1968).
[26] S. Geltman and M. B. Hidalgo, J. Phys. B **4**, 1299 (1971).
[27] A. R. Holt and B. L. Moiseiwitsch, J. Phys. B **4**, 1318 (1971).
[28] M. B. Hidalgo and S. Geltman, J. Phys. B **5**, 627 (1972).
[29] T. C. Wong, J. S. Lee, and R. A. Bonham, Phys. Rev. A **11**, 1963 (1975).
[30] J. F. Ying, T. A. Daniels, C. P. Mathers, H. Zhu, and K. T. Leung, Phys. Rev. A **47**, 5 (1993).
[31] G. E. Chamberlain, J. A. Simpson, S. R. Mielczarek, and C. E. Kuyatt, J. Chem. Phys. **47**, 4266 (1967).
[32] C. E. Kuyatt, *Methods of Experimental Physics*, edited by L. Marton (Academic, New York, 1968), Vol. 7, Pt. A, pp. 11–43.
[33] E. N. Lassettre, J. Chem. Phys. **43**, 4479 (1965); K. N. Klump and E. N. Lassettre, *ibid.* **68**, 886 (1978).
[34] Feng Renfei, Yang Bingxin, Wu Shulan, Xing Shilin, Zhang Fang, Zhong Ziping, and Xu Kezun, Sci. Chin. A (to be published).
[35] G. P. Li, T. Takayanagi, K. Wakiya, H. Suzuki, T. Ajiro, S. Yagi, S. S. Kano, and H. Suzuki, Phys. Rev. A **38**, 1240 (1988).
[36] J. P. Bromberg, J. Chem. Phys. **61**, 963 (1974).
[37] E. N. Lassettre and E. A. Jones, J. Chem. Phys. **40**, 1218 (1964).